

## Research Note

# A current source density analysis of field potentials evoked in slices of visual cortex

K. M. Bode-Greuel<sup>1</sup>, W. Singer<sup>1</sup>, and J. B. Aldenhoff<sup>2</sup>

<sup>1</sup> Max-Planck-Institut für Hirnforschung, Deutschordenstraße 46, Postfach 71 06 62, D-6000 Frankfurt 71, Federal Republic of Germany

<sup>2</sup> Psychiatrische Universitätsklinik, Johannes Gutenberg-Universität, Langenbeckstraße 1, D-6500 Mainz, Federal Republic of Germany

**Summary.** The method of one-dimensional current source density (CSD) analysis was applied to field potentials recorded from 350  $\mu\text{m}$  thick slices of the primary visual cortex of rats and cats. Field potentials were elicited by stimulation of the white matter and recorded along trajectories perpendicular to the cortical layers at spatial intervals of 25 to 50  $\mu\text{m}$ . The resulting CSD distributions resembled closely those recorded from the cat visual cortex "in vivo". The responses with the shortest latency were distinct sinks in layers IV and VI probably reflecting monosynaptic EPSP's from specific thalamic afferents. From layer IV activity was relayed along three major routes: 1. to the supragranular layers via strong local connections to layer III and from there via both short and long range connections to layer II, 2. to targets within layer IV, and 3. to layer V. The source distributions suggest that the projections to layers III and II terminate on the proximal and distal segments, respectively, of apical dendrites of layer III pyramidal cells while the projection to layer V contacts the apical dendrites of layer VI pyramidal cells. These results indicate that all the excitatory pathways that are detectable with the CSD technique in the "in vivo" preparation remain intact in 350  $\mu\text{m}$  thick cortical slices. However, in the slice paired pulse stimulation did not lead to a depression of the response to the second stimulus while this is the case "in vivo". This might be due to reduced inhibition in the slice which has been reported by several authors.

**Key words:** Cortex slices – Field potentials – Current source density analysis – Visual cortex

## Introduction

Cortex slices maintained "in vitro" are commonly used for electrophysiological investigations, because

they have certain advantages over "in vivo" preparations and ideally complement the latter. However, in a slice of 350  $\mu\text{m}$  thickness many neuronal processes are destroyed. For the evaluation of data obtained from slices it is important therefore to determine to what extent the characteristic features of cortical connectivity are preserved.

In order to address this issue we applied the method of current source density (CSD) analysis to electrically evoked field potentials, because this technique enables the assessment of the spatio-temporal pattern of synaptic activity in laminated structures of the CNS (Freeman and Stone 1969; Nicholson and Freeman 1975; Mitzdorf 1985). In slices of the visual cortex of rats and cats we evoked field potentials by white matter stimulation, computed from them the one-dimensional CSD profiles and compared these to those obtained previously in "in vivo" preparations (Mitzdorf and Singer 1978; 1979).

## Methods

For the preparation of rat cortex slices, adult albino rats (140 to 160 g) were anaesthetized with ether, decapitated and the brains removed carefully. Before slicing, the brains were cooled down in 4° C Krebs-Ringer solution. Transverse slices (350  $\mu\text{m}$ ) were cut with a vibratome in the frontal plane. Before recording, the slices were incubated for 1 h in 35  $\pm$  0.5° C Krebs-Ringer solution (in mM: NaCl 124, KCl 5, MgSO<sub>4</sub> 2, Na<sub>2</sub>HPO<sub>4</sub> 1.25, CaCl<sub>2</sub> 2, NaHCO<sub>3</sub> 26, glucose 10) that was saturated with Carbogen (95% O<sub>2</sub>/5% CO<sub>2</sub>). For the preparation of slices from kitten visual cortex the animals were deeply anaesthetized with a mixture of ketamine hydrochloride (35 mg/kg) and xylazine hydrochloride (15 mg/kg), i.m., and mounted in a stereotactic head holder. After craniotomy and resection of the dura mater cardiac arrest was induced by an intravenous injection of a 10% KCl solution in order to reduce bleeding, and immediately thereafter blocks of the visual cortex were removed. The tissue was further processed as described for rat cortex slices.

For recording, the slices were transferred to an interface chamber that was continuously perfused with Krebs-Ringer solution at 35° C. For electrical stimulation of the afferents to striate

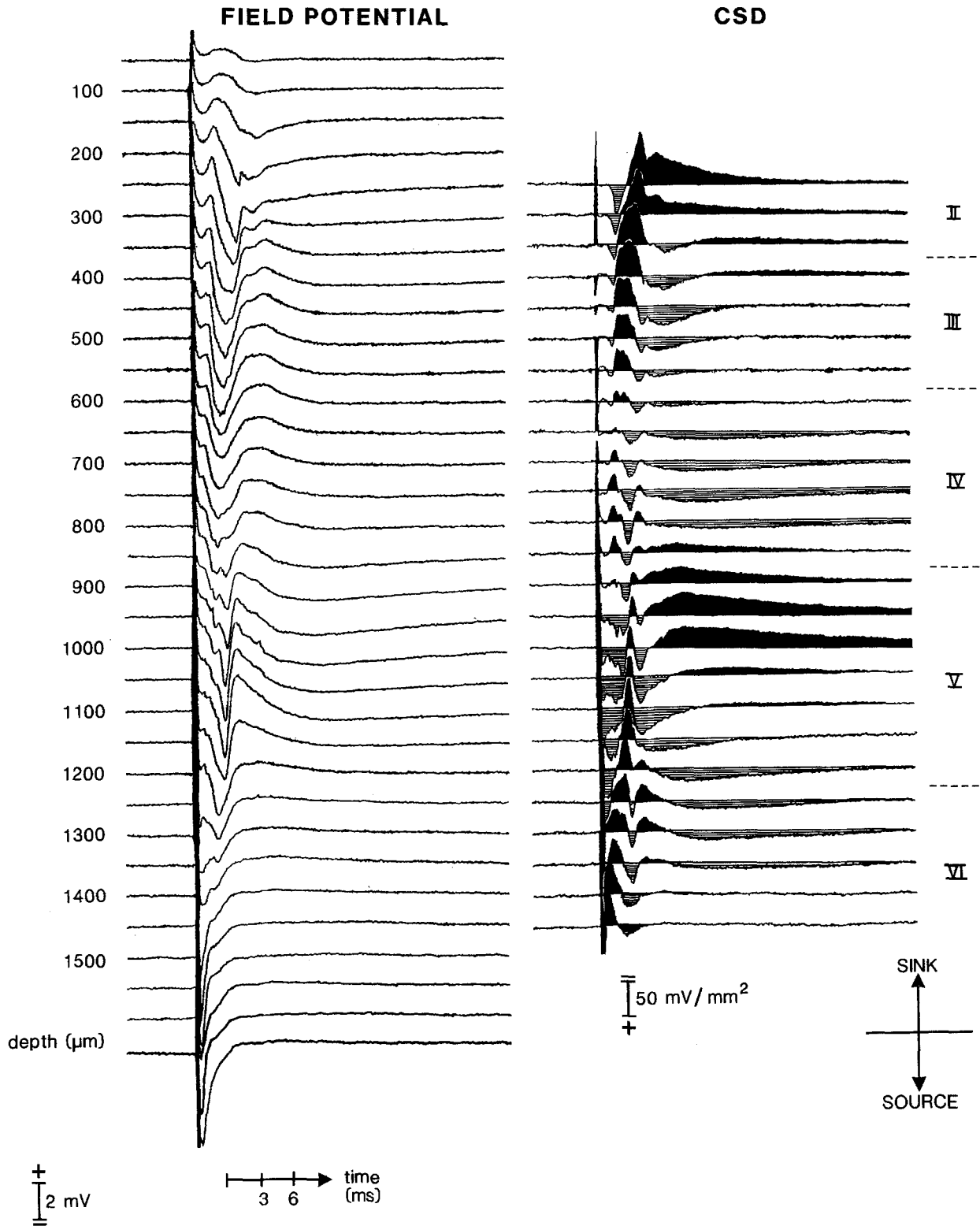


**Fig. 1.** Field potentials (left) recorded from a slice of the primary visual cortex of a 5-week-old kitten and corresponding CSD distributions (right). The sinks which represent the sites of inward currents are filled black and the sources reflecting outward currents are hatched horizontally. At the right margin the borders of the cortical laminae are indicated. Because field potential measurements were started only 50 μm below the pial surface and because we used a differentiation grid of 200 μm, CSD profiles from layer I are missing

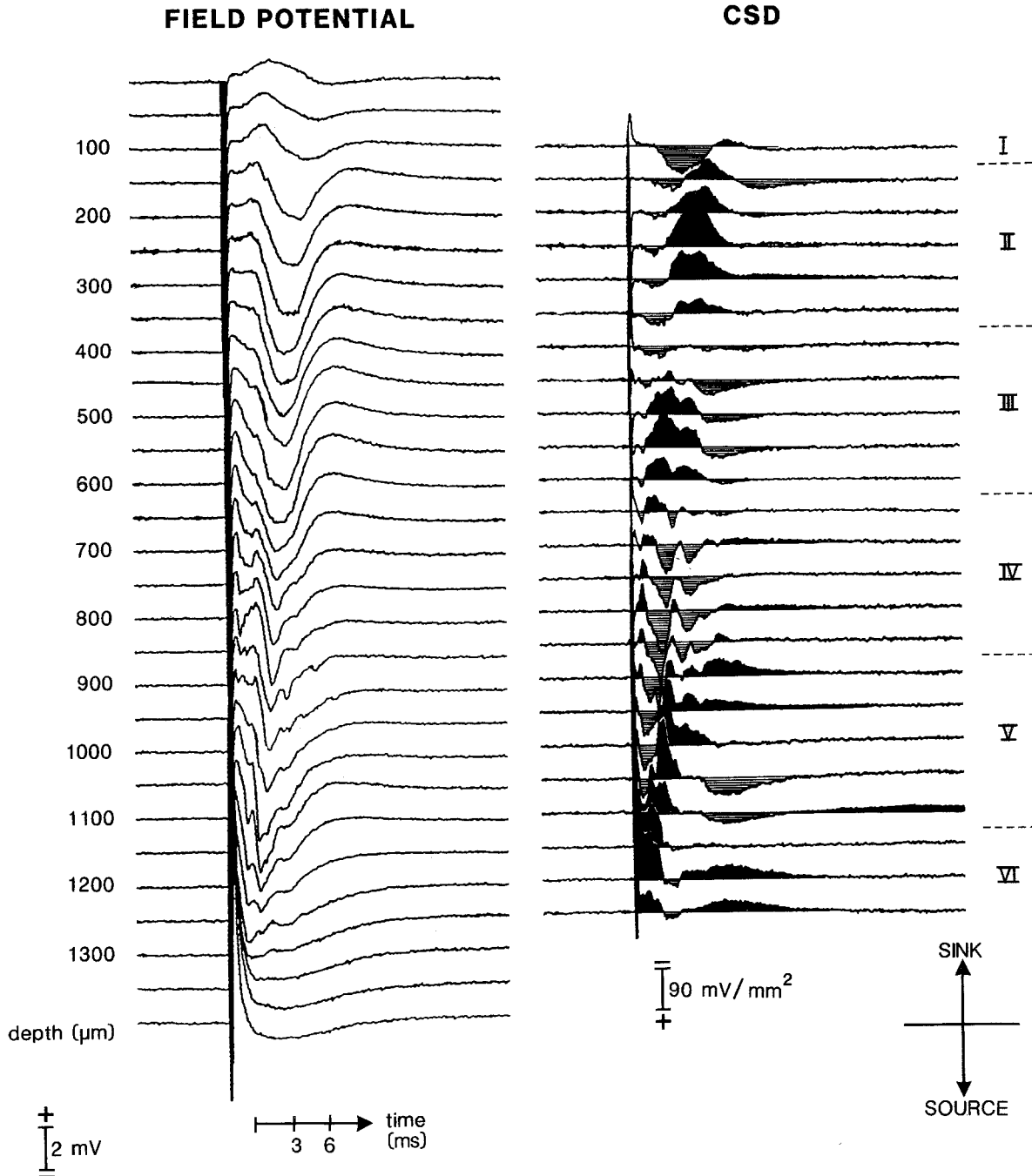


**Fig. 2.** Field potentials (left) recorded from a slice of the primary visual cortex of a rat and corresponding CSD distributions (right). Conventions as in Fig. 1. The differentiation grid was 150  $\mu\text{m}$ . The first CSD profile was obtained by applying a differentiation grid of 100  $\mu\text{m}$ . Thus, a large source which is typical for layer I could be visualized

cortex a bipolar stimulation electrode was placed in the white matter subjacent to the recording sites. Square wave pulses of 50  $\mu\text{s}$  duration were applied at 0.1 Hz. Extracellular field potentials were recorded with glass micropipettes (1–10  $\text{M}\Omega$ ) at a depth of 100  $\mu\text{m}$  from the surface of the slice along trajectories orthogonal to the cortical laminae at intervals of 25 or 50  $\mu\text{m}$ . The stimulus intensity was adjusted to elicit a near-maximal response. The experiment was started once the field response had become stable for at least 15 min. Signals were recorded differentially

between the microelectrode and an indifferent electrode in the bath using a FET equipped head stage (impedance  $10^{12} \Omega$ ) with conventional capacity compensation. After further amplification the signals were band pass-filtered from 1 Hz to 3 kHz and digitized at a rate of 10 kHz. At each recording site 10 consecutive responses were averaged and stored on disk. From the sets of 30 to 45 field potentials per trajectory, CSD profiles were computed according to the method described by Mitzdorf and Singer (1978) and Mitzdorf (1985). The computational algorithm is based on the

assumption that the extracellular space has the properties of an Ohmic conductor and that the electrical fields are quasi-static. In this case extracellular current densities are linearly related to the spatial gradients of the field potentials, the former being extractable from the latter by simple differentiation. Since in the cerebral cortex, the field potentials are translationally invariant in the two dimensions parallel to the cortical layers and show distinct changes only perpendicular to the layers (Mitzdorf and Singer 1978) the one-dimensional CSD method was applied. The second spatial derivatives of the potentials were calculated according to the formula:

$$\frac{\partial^2 \Phi}{\partial z^2} \approx \frac{\Phi(z+n \cdot \Delta z) - 2\Phi(z) + \Phi(z-n \cdot \Delta z)}{(n \cdot \Delta z)^2}$$

where  $\Phi$  is the extracellular field potential,  $z$  is the coordinate perpendicular to the laminae,  $\Delta z$  is the sampling interval,  $n \cdot \Delta z$  is the differentiation grid. In one experiment the CSD pattern was related to the cortical laminae by comparing the location of the field potentials to the location of dye marks that were deposited from the microelectrode during recording and retrieved subsequently in the Nissl-stained slice.

## Results

Twelve sets of field potentials obtained from slices of 10 rats, 1 cat and 1 kitten, were subjected to a CSD analysis. The resulting CSD patterns showed only minor variations in different experiments. The comparison of the location of dye marks with the CSD patterns allowed to attribute individual current sinks and sources to particular cortical layers.

In the following, three representative CSD patterns are documented. The first is from a slice of area 17 of a 5-week-old kitten and allows a direct comparison with CSD patterns obtained from cats *in vivo* (Mitzdorf and Singer (1978)). The second and third examples show CSD distributions in the primary visual cortex of adult rats after single and paired pulse stimulation, respectively.

The field potential and CSD distributions in the slice of the kitten visual cortex are shown in Fig. 1. The earliest postsynaptic response component in the CSD pattern is a sink with a peak latency of 1.5 ms. It extends over a depth of 0.7 to 0.85 mm below the pial surface which corresponds to layer IV. It is followed with a delay of 0.7 ms by a larger sink which extends from 0.4 to 0.6 mm below the surface and is thus confined mainly to layer III. This sink merges with a more delayed sink that extends further up towards the pial surface and starts with a delay of 0.9 ms (2.7 ms poststimulus) after the layer III sink. Both the latency and duration of this sink increase continuously with decreasing distance from the pial surface. At a depth of 0.25 mm this sink has a peak latency of 3.9 ms and a duration of more than 40 ms. At a depth of 0.9 to 1.2 mm which corresponds to layer V, a large and well defined sink occurs with an

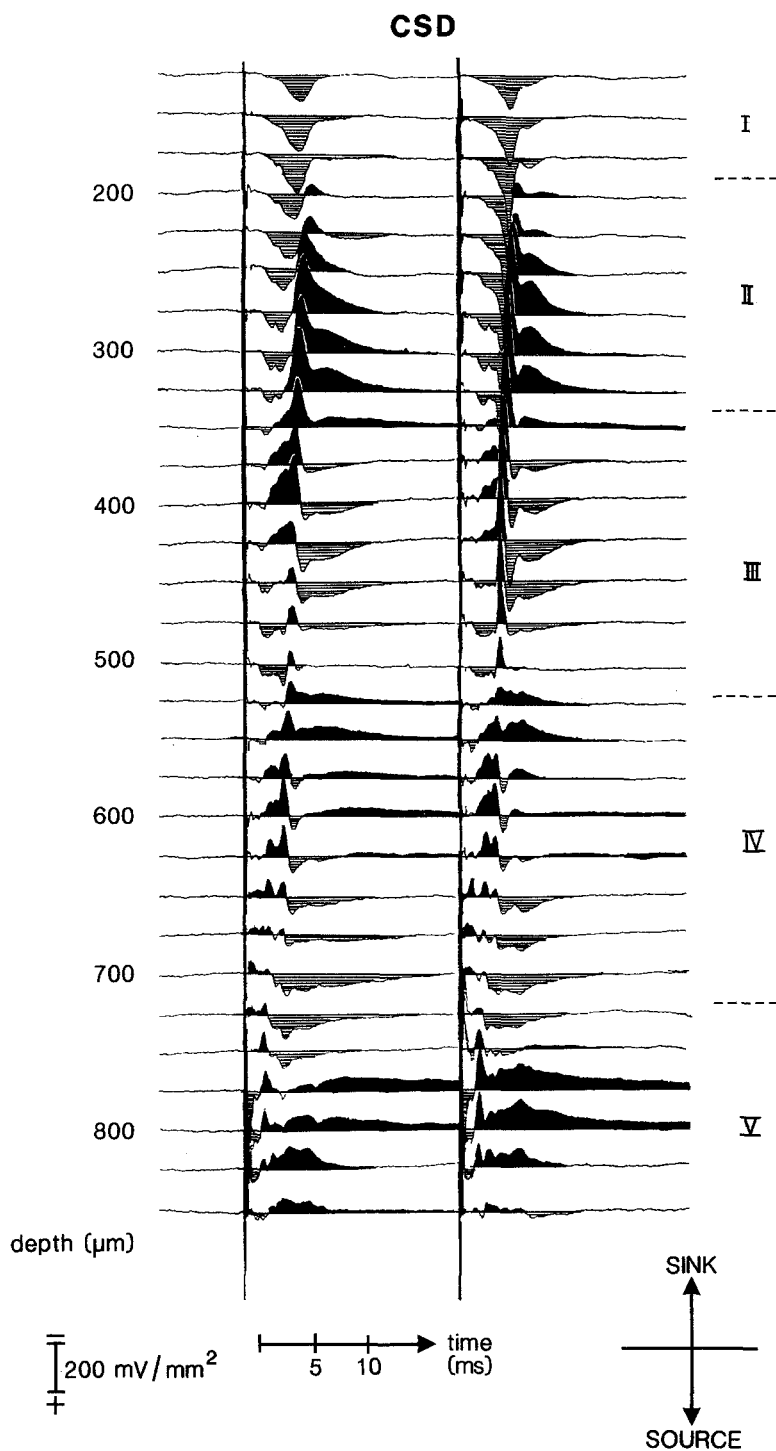
onset latency of about 2.5 ms. In the superficial part of layer V, immediately adjacent to layer IV, this sink is followed by a second, very prolonged sink that lasts for more than 40 ms. At a depth of 1.25 mm and more, which corresponds to layer VI, another short latency sink is disclosable whose latency decreases with increasing depth and is in the range of the early sink in layer IV. This deep sink is split in two components by a source which is most likely associated with the early sink in layer V.

Figure 2 shows field potentials (left) and corresponding CSD distributions from a cortex slice of an adult rat. In general, the CSD pattern is similar to that obtained in the kitten and cat slices. The earliest sink in the CSD profiles starts 0.8 ms after the stimulus and extends over a depth of 0.65 to 0.9 mm below the pial surface which corresponds to layer IV. With a delay of 0.9 ms another sink is discernable in a depth of 0.45 to 0.65 mm from pial surface which corresponds to layer III. This sink is followed with a delay of 1.7 ms by another large sink which is located essentially in layer II. The current sinks in the supragranular layers are both strong but the sink in layer II is not biphasic and not as long-lasting as in the kitten CSD presented above. The response in layer V (0.9 mm to 1.1 mm from the pial surface) has an onset latency of 2.5 ms and is biphasic as the layer V response of the kitten slice. A large short latency sink can also be detected in layer VI probably reflecting again monosynaptic input to layer VI. The very early sinks in lower layer VI merge with the stimulation artifact.

Figure 3 shows the response of a visual cortex slice of an adult rat to double-shocks that were separated by 20 ms and repeated once every 10 s. The CSD patterns elicited by both stimuli resemble closely those shown in Figs. 1 and 2. The only difference is that the responses to the second stimulus are somewhat larger and of shorter latency than those to the first stimulus. This is true for the responses in all layers. In layer IV this enhancement accentuates a delayed sink. When the stimulation paradigm was changed from single pulse to paired pulse stimulation, the response to the first stimulus was depressed initially and increased after 3 to 5 stimuli above control level. This effect persisted even if the intervals between the pulse pairs exceeded 20 s.

## Discussion

The CSD patterns obtained after white matter stimulation from slices of the rat and cat visual cortex closely resembled each other, confirming the notion that the basic principles of connectivity are similar in



**Fig. 3.** Current source density distribution in a slice of the primary visual cortex of a rat, evoked by double-shock stimuli of 20 ms intervals. The responses to the second stimulus are larger and of shorter latency than those to the first stimulus. Conventions as in Fig. 1. The differentiation grid was 100  $\mu\text{m}$

the visual cortices of the two species. Moreover, these CSD profiles were very similar to those measured by Mitzdorf and Singer (1978, 1979) in the cat and the monkey visual cortex "in vivo". This supports the conjecture that the one-dimensional CSD analysis is applicable to thin cortical slices. The altered geometry of the conductive environment and

the more focal stimulation do not seem to interfere to any substantial extent with the local fields from which we computed our CSD patterns. Moreover, the similarity between the "in vivo" and "in vitro" patterns indicates that those excitatory pathways that can be disclosed with the CSD method are preserved in the slice preparation.

As has been discussed in detail by Mitzdorf (1985) it is possible to infer from the latencies of sinks and sources and from their spatial pattern the flow of excitation in cortical circuits. However, for an unambiguous interpretation the conduction velocities of the afferent pathways need to be known in addition. In the present experiments these were not measured, but because of the short conduction distance different conduction velocities would introduce variations in response latency that are small compared to those caused by synaptic delays. We therefore interpret the present CSD patterns following the arguments of Mitzdorf and Singer (1978).

The sinks in layer III were delayed by about 0.8 ms with respect to the monosynaptic sinks in layer IV, suggesting that they result from a synaptic response to afferents originating in layer IV. The sinks draw their current mainly from above which indicates that the respective target profiles extend through layers III and II and receive their excitatory input at the lower third of their extent. This identifies the apical dendrites of layer III pyramidal cells as the most likely targets of the pathway from layer IV to layer III. The sinks in layer II started 0.9 ms to 1.6 ms after the sink in layer III and therefore reflect most likely another synaptic step within the supragranular pathway. The large amplitudes of these sinks indicate that the connections to layer II are rather strong. The long duration of this superficial sink may have several reasons. It could result from convergence of pathways with additional synaptic delays or from pathways with slow conduction velocities. It could also reflect the absence of events which normally antagonize inward currents such as action potentials or IPSP's. The duration of the superficial sink was variable from slice to slice. This might reflect variations in global excitability but it could also be due to changes in the angle at which the slices were cut. Since tangential intracortical connections are anisotropic the extent of their preservation depends critically on the plane of the section. The sources corresponding to the sinks in layer II are mainly in layer III. This implies that the prominent targets of this polysynaptic activity are again the apical dendrites of layer III pyramidal cells.

The latencies of the early infragranular current sinks in layer V suggest a disynaptic excitatory input from layer IV to layer V. The late and very long-lasting sinks in layer V could again result from polysynaptic pathways or from connections with slow conduction velocity. Both early and late sinks drew current from above and from below. The profiles generating the layer V sinks are therefore most likely layer VI pyramidal cells that are contacted by excitatory synapses at the middle parts of their apical dendrites.

The short latency sinks in layer VI had a similar latency as the layer IV sinks and therefore resulted most likely from the primary afferents that terminate in this layer. The related sources were above the sinks indicating that the corresponding synapses are located on soma-near dendrites of layer VI pyramidal cells. The sinks in lower layer VI had latencies too short to be compatible with a synaptic origin and as has been inferred from the *in vivo* preparation (Mitzdorf and Singer 1978) reflect most likely the activity in bifurcating subcortical afferents.

#### *Differences between in vitro and in vivo preparations*

One difference between the "in vivo" and the "in vitro" preparation concerns the monosynaptic current sinks in layer IV. The geniculate afferents to area 17 of the cat consist of two distinct populations, the X- and Y-axons, that differ with respect to their conduction velocities (Hoffman and Stone 1971) and laminar termination patterns (LeVay and Gilbert 1976; Mitzdorf and Singer 1978). These two populations can be resolved in the CSD patterns of the "in vivo" but not of the slice preparation. The reason is that in the latter case the stimuli are delivered in such close proximity to the cortex that the small differences in conduction velocity are no longer detectable.

Another difference between "in vitro" and "in vivo" responses was that in the slice paired pulse stimulation did not lead to a depression of the response to the second stimulus while such occurs consistently "in vivo" (Mitzdorf and Singer 1978). One reason for this might be reduced inhibition in the slice. Corresponding reports have been published by Connors et al. (1982) and McCormick et al. (1985) who only rarely observed inhibitory postsynaptic potentials (IPSP's) in cortex slices. In some cells they could evoke a long-lasting hyperpolarizing IPSP that was easily reduced by stimulation at frequencies higher than 0.2 Hz. While it is not obvious why local inhibitory circuits should be more impaired by slicing than excitatory connections there are reports which suggest that the small inhibitory neurons are especially sensitive to mechanical damage and hypoxia (Alger et al. 1984). However, this interpretation may not suffice to account for the observation that the response to the second stimulus was enhanced after repeating the pulse pairs several times. The possibility should be considered therefore that additional short-term potentiation effects contribute to paired-pulse facilitation which do not manifest themselves in the "in vivo" preparation.

The fact that in the slice, white matter stimulation elicits essentially the same pattern of intracortical

activity as the *in vivo* stimulation of the specific retinal afferents has several important implications: First, it suggests that slice preparations are ideally suited not only for the analysis of single cell properties but also for a detailed analysis of the flow of specific input signals through cortical circuitry. Second, since there is a good correlation between single unit responses, CSD distributions and field potentials “*in vivo*” (Neumann 1981, thesis), field potentials and CSD analyses can in the future be used also in the cortex slice to assess the responses of distinct cell populations. Finally, since the CSD profiles obtained “*in vivo*” by stimulation of the optic nerve are similar to those elicited “*in vitro*” by stimulation of the white matter it can be concluded that the resolvable activation pattern in the slice preparation mainly results from the activation of specific visual afferents. This facilitates a correlation of data obtained from “*in vivo*” and “*in vitro*” experiments. In conclusion, the present results emphasize that electrophysiological data from slice experiments can be generalized to the “*in vivo*” preparation which supports further the validity of the “*in vitro*” preparation.

*Acknowledgements.* We wish to thank Mr. G. Bink for technical assistance, Ms. R. Ruhl for preparing the figures, and Ms. G. Trauten-Luhmann for editing the manuscript.

## References

- Alger BE, Dhanjal SS, Dingledine R, Garthwaite J, Henderson G, King GL, Lipton P, North A, Schwartzkroin PA, Sears TA, Segal M, Wittingham TS, Williams J (1984) Brain slice methods. In: Dingledine R (ed) Brain slices. Appendix. Plenum Press, New York, p 401
- Connors BW, Gutnick MJ, Prince DA (1982) Electrophysiological properties of neocortical neurons *in vitro*. *J Neurophysiol* 48: 1302–1320
- Freeman JA, Stone J (1969) A technique for current source density analysis of field potentials and its application to the frog cerebellum. In: Llinás R (ed) Neurobiology of cerebellar evolution and development. American Medical Association, Chicago, pp 421–430
- Hoffmann KP, Stone J (1971) Conduction velocity of afferents to cat visual cortex: a correlation with cortical receptive field properties. *Brain Res* 32: 460–466
- LeVay S, Gilbert CD (1978) Laminar patterns of geniculocortical projections in the cat. *Brain Res* 113: 1–19
- McCormick DA, Connors BW, Lighthall JW, Prince DA (1985) Comparative electrophysiology of pyramidal and sparsely spiny stellate neurons of the neocortex. *J Neurophysiol* 54: 782–806
- Mitzdorf U (1985) Current source density method and application in cat cerebral cortex: investigations of evoked potentials and EEG phenomena. *Physiol Rev* 65: 37–100
- Mitzdorf U, Singer W (1978) Prominent excitatory pathways in the cat visual cortex (A 17 and A 18): a current source density analysis of electrically evoked potentials. *Exp Brain Res* 33: 371–394
- Mitzdorf U, Singer W (1979) Excitatory synaptic ensemble properties in the visual cortex of the macaque monkey: a current source density analysis of electrically evoked potentials. *J Comp Neurol* 187: 71–84
- Neumann G (1981) Zur Organisation der intracorticalen Verschaltung in der Sehrinde. Doctoral Thesis. Technical University, Munich
- Nicholson C, Freeman JA (1975) Theory of current source density analysis and determination of conductivity tensor for Anuran cerebellum. *J Neurophysiol* 38: 356–368

Received May 19, 1987 / Accepted August 26, 1987